Mon. Not. R. Astron. Soc. **278,** 395–405 (1996)

Cooperation of orbital streams in disc galaxies

David J. D. Earn[1,2]★ and D. Lynden-Bell[1]★

[1] *Institute of Astronomy, Madingley Road, Cambridge CB3 0HA*
[2] *The Racah Institute of Physics, The Hebrew University, Jerusalem 91904, Israel*

Accepted 1995 July 28. Received 1995 July 10; in original form 1995 January 9

ABSTRACT

An orbit is said to cooperate with a potential well if it tends to deepen it by aligning with it. We derive analytical formulae that give the response of resonant orbits to non-axisymmetric perturbations. This makes it possible to quantify the level of cooperation in a given galaxy model. The qualitative response of orbits can be characterized by the sign of what we call the cooperation parameter. We discuss the relevance of our results for theories of the formation and maintenance of bars and lopsidedness.

Key words: instabilities – celestial mechanics, stellar dynamics – galaxies: kinematics and dynamics – galaxies: structure.

1 INTRODUCTION

Disc galaxies may be roughly axisymmetric, but their beauty is mostly a result of the spectacular non-axisymmetric patterns that are seen in light from bright stars and gas. Perhaps the most natural question to ask is whether these patterns, such as bars and spirals, are transient or long-lived. If they are transient they must recur frequently, since they are observed in most discs, but it is difficult to say more with certainty. It is fairly clear that the observed asymmetries are manifestations of density waves, but there is no general agreement on the origin and lifetime of these phenomena (for background see Binney & Tremaine 1987).

The orbital period of a typical star is much shorter than the time over which an overall galactic pattern changes. It is therefore possible to ignore the motions of individual stars and consider only the behaviour of *streams* of stars along given galactic orbits. We may then ask how a given orbital stream responds to the presence of a non-axisymmetric perturbation in the disc. Does it tend to align with the density enhancement and thus *cooperate* with the formation or maintenance of a pattern? Or does the orbital stream react by increasing its distance from the density peak? These are the questions we address in this paper.

Lynden-Bell (1979) introduced the notion of cooperation of orbital streams (without using this term) when he considered a possible formation mechanism for galactic bars. We consider more generally the response of orbital streams to patterns of any given azimuthal wavenumber, and we make a point of emphasizing lopsided ($m=1$) patterns, which are very common in disc galaxies but have received little attention.

★ E-mail: earn@astro.huji.ac.il; dlb@ast.cam.ac.uk

What we shall call the *cooperation parameter* ζ is in more abstract settings often called the *non-linearity parameter* (e.g., Lichtenberg & Lieberman 1992, section 2.4a). We shall stick to the former term, since it expresses the physical motivation of our work.

In Section 2 we introduce our notation and give a qualitative discussion of the cooperation mechanism (a more rigorous and complete discussion is given by Earn 1993). Our main results, including a general formula for the cooperation parameter for nearly circular orbits in an arbitrary axisymmetric disc, are presented in Section 3. Implications of our results are discussed in Section 4. In particular, based on analytical results derived here and simulations reported elsewhere, we argue *against* Lynden-Bell's (1979) original proposal that the linear bar instability of stellar discs is driven by cooperative alignment of orbits. Instead, we believe that the cooperation mechanism is effective mainly for the *non-linear* evolution of discs and may govern the *maintenance* of non-axisymmetric patterns.

2 BASIC CONCEPTS AND NOTATION

2.1 α-symmetry

Consider a star with angular frequency Ω and radial frequency κ in an axisymmetric disc galaxy. As seen from axes rotating with angular velocity Ω_a, the star goes around the galaxy in the period $2\pi/(\Omega-\Omega_a)$. It goes in and out in the period $2\pi/\kappa$. Therefore the orbit as thus seen will close with m lobes after ℓ turns if

$$m\frac{2\pi}{\kappa}=\ell\frac{2\pi}{\Omega-\Omega_a}. \tag{2.1}$$

Four lobes can be produced after two turns only if there are two lobes after one turn, etc., so we may always assume that

m and ℓ are relatively prime. If we write

$$\alpha = \frac{m}{\ell}, \tag{2.2}$$

then equation (2.1) can be written as

$$\Omega_\alpha = \Omega - \frac{1}{\alpha}\kappa. \tag{2.3}$$

For large α there are many lobes after a single turn. $\alpha \to \infty$ gives uniform rotation. Ω_α is well defined even if α is irrational, but the orbit closes only in the rational case (see Binney & Tremaine 1987, fig 6-9 for examples with $\alpha = \infty$, 2, -2 and 3/2).

We say that an orbit is m/ℓ-symmetric or α-symmetric in a given rotating frame if it closes with m lobes after ℓ turns around the origin relative to that frame. We say that a pattern is α-symmetric if it is made up of α-symmetric orbits.

2.2 Cooperation

Suppose that a nearly axisymmetric galaxy is perturbed by a lopsided density wave, as indicated schematically in Fig. 1. The orbits drawn as solid curves form part of the lopsided perturbation. These orbits are imagined to be stationary in the figure, i.e., they all close with $\alpha = 1$ symmetry in the frame rotating with the perturbation at the rate $\Omega_p < 0$ (the pattern rotates clockwise in an inertial frame).

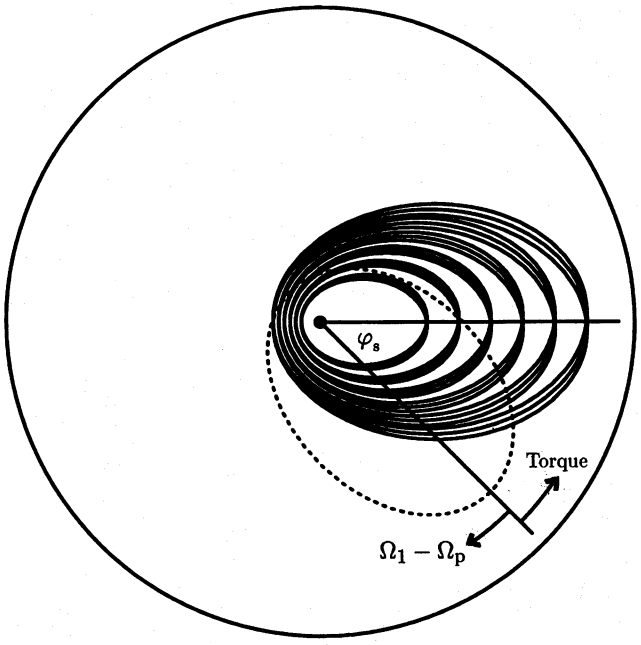

Figure 1. The mechanism of cooperation of orbital streams, presented schematically for the lopsided ($\alpha = 1$) resonance. An $\alpha = 1$ symmetric 'test orbital stream' (dotted curve) is shown interacting with a lopsided density enhancement, which is displayed as a selection of nearly aligned $\alpha = 1$ symmertric orbits. The motion is shown in the frame rotating at the pattern rotation rate $\Omega_p < 0$, so the density perturbation is not rotating in this figure. The test orbital stream is precessing at the rate $\Omega_1 - \Omega_p = |\Omega_p| - |\Omega_1|$, which is presumed to be slow. If the cooperation parameter ζ is positive then the torque will tend to align the test orbital stream with the density perturbation.

The dotted orbit closes with $\alpha = 1$ symmetry in a frame rotating at the rate $\Omega_1 < 0$, which differs no more than slightly from Ω_p, so the precession rate, $\Omega_1 - \Omega_p = -|\Omega_1| + |\Omega_p|$, of the dotted orbit relative to the perturbation is small. In Fig. 1, $\Omega_1 - \Omega_p$ is assumed to be negative (clockwise precession), but it could equally well be positive.

A star on the dotted orbit feels torques from the pattern potential at approximately the same orbital phase each time it goes around the galaxy; since the dotted orbit is not aligned with the lopsided pattern these torques add up over several orbital times. Thus the interaction is significant and will change the orbital alignment. Which way will the dotted orbit go?

The answer to this question is not obvious, because the interaction we are considering is viewed in a rotating frame of reference. The dotted orbit can in fact go either way, depending on the structure of the unperturbed axisymmetric potential.

The reader may wonder whether it makes sense to talk about 'the dotted orbit' in the first place. We are assuming that the shape of the orbit does not change significantly during the interaction. Might not the dotted orbit be completely disrupted by the perturbation?

To be sure that this is not the case we have made three assumptions: (i) the amplitude of the perturbation in potential is small, (ii) the period of the dotted orbits is small compared with its precession rate relative to the rotating perturbation, and (iii) the dotted orbit is near resonance with the perturbation, i.e., $|\Omega_1 - \Omega_p|/\Omega_p \ll 1$. These reasonable assumptions justify averaging over the fast motion of the star around its orbit and focusing on changes in orbital alignment.

There is nothing special about the lopsided $\alpha = 1$ resonance in this discussion. We could equally well have drawn a perturbation and orbits with any α-symmetry. [The $\alpha = 2$ case ($m = 2$, $\ell = 1$) is discussed in Lynden-Bell (1979).] Formally, averaging over the fast motion of the stars yields an exactly constant 'fast action',

$$J_f = J_R + \frac{1}{\alpha} J_\phi = J_R + \frac{\ell}{m} h, \tag{2.4}$$

where $J_\phi = h$ is the angular momentum (azimuthal action) and $J_R = (1/2\pi)\oint p_R \, dR$ is the radial action (we denote by φ_ϕ and φ_R the angles conjugate to J_ϕ and J_R respectively). Thus the averaging procedure gives a reliable result only if J_f is roughly constant (adiabatically invariant) as the perturbation grows; we expect this to be the case in galaxies. The angle variable conjugate to J_f is φ_R, the angle conjugate to J_R, but we denote it as φ_f in order to be clear which set of variables is in use. There is also an action associated with the slow motion, i.e., the precession of the axes in which the orbit closes. This 'slow action' is $J_s = J_\phi = h$; it *does* change. (Recall that angular momentum is strictly conserved for an orbit in an axisymmetric potential, so changes in h are due entirely to the non-axisymmetric disturbances. See Lynden-Bell & Kalnajs 1972 for a discussion of angular momentum exchange.) The angle φ_s, conjugate to the action J_s, determines the orientation of the lobe of the 'test orbital stream' (the dotted orbit in Fig. 1).

Returning to Fig. 1, stars on the dotted orbit stream forward (counter-clockwise) in an inertial frame, so they

appear to stream faster forwards in the backward-rotating frame depicted (galactic orbits typically complete one radial oscillation in less than one azimuthal period, so the frame needs to rotate backwards to cause orbits to close with $\alpha = 1$ symmetry). The torque from the potential trough therefore tugs streaming stars in the direct sense (counter-clockwise) and thereby increases their angular momentum h. If $|\Omega_1|$ decreases as h increases, then $\Omega_1 - \Omega_p = |\Omega_p| - |\Omega_1|$ increases and the orbit as a whole is pulled towards the pattern and tends to align with it; on the other hand, if $|\Omega_1|$ *increases* as h increases, then the orbit will be pushed away from the pattern. Since Ω_1 is negative this condition for trapping or *cooperation* of orbits is

$$\zeta \equiv \left(\frac{\partial \Omega_\alpha}{\partial h}\right)_{J_f} > 0, \tag{2.5}$$

where we have used a general α since the condition is the same for a configuration with any given α-symmetry (the adiabatic invariant J_f is different for different α; equation 2.4). The lobe angular velocity Ω_α can itself be written in terms of the unperturbed Hamiltonian H for the underlying axisymmetric disc:

$$\Omega_\alpha = \frac{\partial H}{\partial J_s} = \left(\frac{\partial H}{\partial h}\right)_{J_f}. \tag{2.6}$$

We may therefore write the cooperation parameter as

$$\zeta = \left(\frac{\partial^2 H}{\partial h^2}\right)_{J_f}. \tag{2.7}$$

The assumption of adiabatic invariance of J_f is valid because the potential changes only as fast as orbits are trapped, which happens slowly compared with an orbital time.

This qualitative derivation of the cooperation parameter ζ can be made completely rigorous using standard secular perturbation theory (e.g., Born 1927; Goldstein 1980; Arnold 1988, 1989; Lichtenberg & Lieberman 1992, section 2.4a). A full treatment beginning from first principles of Hamiltonian mechanics and focusing on the particular problem of disc galaxy dynamics is given by Earn (1993).

3 WHICH RESONANCES ARE COOPERATIVE?

We have seen that orbital streams behave cooperatively if the cooperation parameter (equations 2.5 and 2.7) is positive. For any given axisymmetric potential $U(R)$ and any resonance α it is possible to compute ζ, at least approximately. In this section we compute ζ exactly for the generalized isochrone potential and give a formula, equation (3.25), for the leading-order term in general. We apply this formula to power laws in Section 3.3 and to another special class of potentials in Section 3.4.

One general observation that can be made is that the corotation resonance ($\alpha = \infty$) will never be cooperative in galaxies: Ω always decreases with h at constant J_R, so $\zeta = (\partial \Omega_\infty / \partial h)_{J_R} < 0$. Cooperation typically occurs for resonant orbits of different type in different ranges of angular momentum.

3.1 Cooperation in the generalized isochrone

In order to calculate ζ exactly, we must be able to write the Hamiltonian H as a function of h and J_f. This can be done if J_R can be computed as a function of h and the energy E. An important non-trivial model for which J_R can be computed analytically is the isochrone (Hénon 1959), which is defined by the potential

$$U(R) = -\frac{GM}{b + \sqrt{R^2 + b^2}}. \tag{3.1}$$

The isochrone gets its name from the property that all orbits of a given energy have the same period, independent of angular momentum; it is a generalization of a point mass ($b = 0$) and a harmonic oscillator ($b \to \infty$). The generalized isochrone (e.g., Evans et al. 1990) has $U_G = U - (1/2)kR^{-2}$, where k can in principle have either sign but is positive if circular orbits near the centre are to be stable. The radial action is

$$J_R = \frac{GM}{\sqrt{-2E}} - \frac{1}{2}(h + \sqrt{h^2 + 4GMb}), \tag{3.2}$$

for the isochrone, and is readily generalized by replacing h by $\sqrt{h^2 + k}$ for the generalized isochrone. For both we can write

$$H = E = \frac{-(GM)^2}{2[J_R + K(h)]^2}, \tag{3.3}$$

where

$$K(h) = \frac{1}{2}(\sqrt{h^2 + k} + \sqrt{h^2 + k_1}), \tag{3.4}$$

and $k_1 = 4GMb + k$. For the isochrone, $k = 0$. The lobe angular velocity of an orbit that closes with m lobes after ℓ turns is ($\alpha = m/\ell$)

$$\begin{aligned}\Omega_\alpha &= \left(\frac{\partial H}{\partial h}\right)_{J_f} = \left(\frac{\partial H}{\partial h}\right)_{J_R} - \frac{1}{\alpha}\left(\frac{\partial H}{\partial J_R}\right)_h \\ &= \frac{(GM)^2}{(J_R + K)^3}\left(K' - \frac{1}{\alpha}\right),\end{aligned} \tag{3.5}$$

and the cooperation parameter is

$$\begin{aligned}\zeta &= \left(\frac{\partial \Omega_\alpha}{\partial h}\right)_{J_f} = \left(\frac{\partial \Omega_\alpha}{\partial h}\right)_{J_R} - \frac{1}{\alpha}\left(\frac{\partial \Omega_\alpha}{\partial J_R}\right)_h \\ &= \frac{-3(GM)^2}{(J_R + K)^4}\left[\left(K' - \frac{1}{\alpha}\right)^2 - \frac{1}{3}K''(J_R + K)\right].\end{aligned} \tag{3.6}$$

Hence orbits in the isochrone are cooperative ($\zeta > 0$) only when $(K' - 1/\alpha)^2 < (1/3)K''(J_R + K)$.

For any given resonance, specified by $\alpha = m/\ell$, there is a range of J_R and h over which such orbits are cooperative, given by

$$M_- < \alpha < M_+, \tag{3.7}$$

where

$$M_{\pm}=\frac{1}{K'\mp\sqrt{(1/3)(J_R+K)K''}}. \tag{3.8}$$

(We cast it in this form to see the connection to the similar condition 3.26 discussed below for power-law potentials.) Now

$$K'=\frac{1}{2}\left(\frac{h}{\sqrt{h^2+k}}+\frac{h}{\sqrt{h^2+k_1}}\right), \tag{3.9}$$

and

$$K''=\frac{1}{2}\left(\frac{k}{(h^2+k)^{3/2}}+\frac{k_1}{(h^2+k_1)^{3/2}}\right)>0. \tag{3.10}$$

Hence, as $h\to\infty$, $K'\to 1$ and $K''K\to 0$. From (3.7) these limits imply that $\zeta<0$ as $h\to\infty$ unless $\alpha=1$. For $\alpha=1$, $\zeta\to(1/2)h^{-2}(1+J_R/h)+\mathcal{O}(h^{-4})$, so for this case ζ is positive showing cooperative behaviour in the outer parts. More generally, (3.7) gives the range over which any given resonance is cooperative. Note that for the isochrone itself ($k=0$)

$$M_{\pm}=\frac{2}{1+h_0/h_1\mp\sqrt{(1/3)h_1^{-3}[h_1+h_0(1+2J_R/h)]}}, \tag{3.11}$$

where $h_0=h/(4GMb)$ and $h_1=\sqrt{1+h_0^2}$. The loci $M_{\pm}$ of vanishing ζ for the isochrone are shown in the main plot of Fig. 2; the inlayed plot shows ζ as a function of h for fixed E and various α. In the limits $b\to 0$ and $b\to\infty$, one finds $M_-=M_+$, so neither the Kepler problem nor the simple harmonic oscillator has any cooperative resonances.

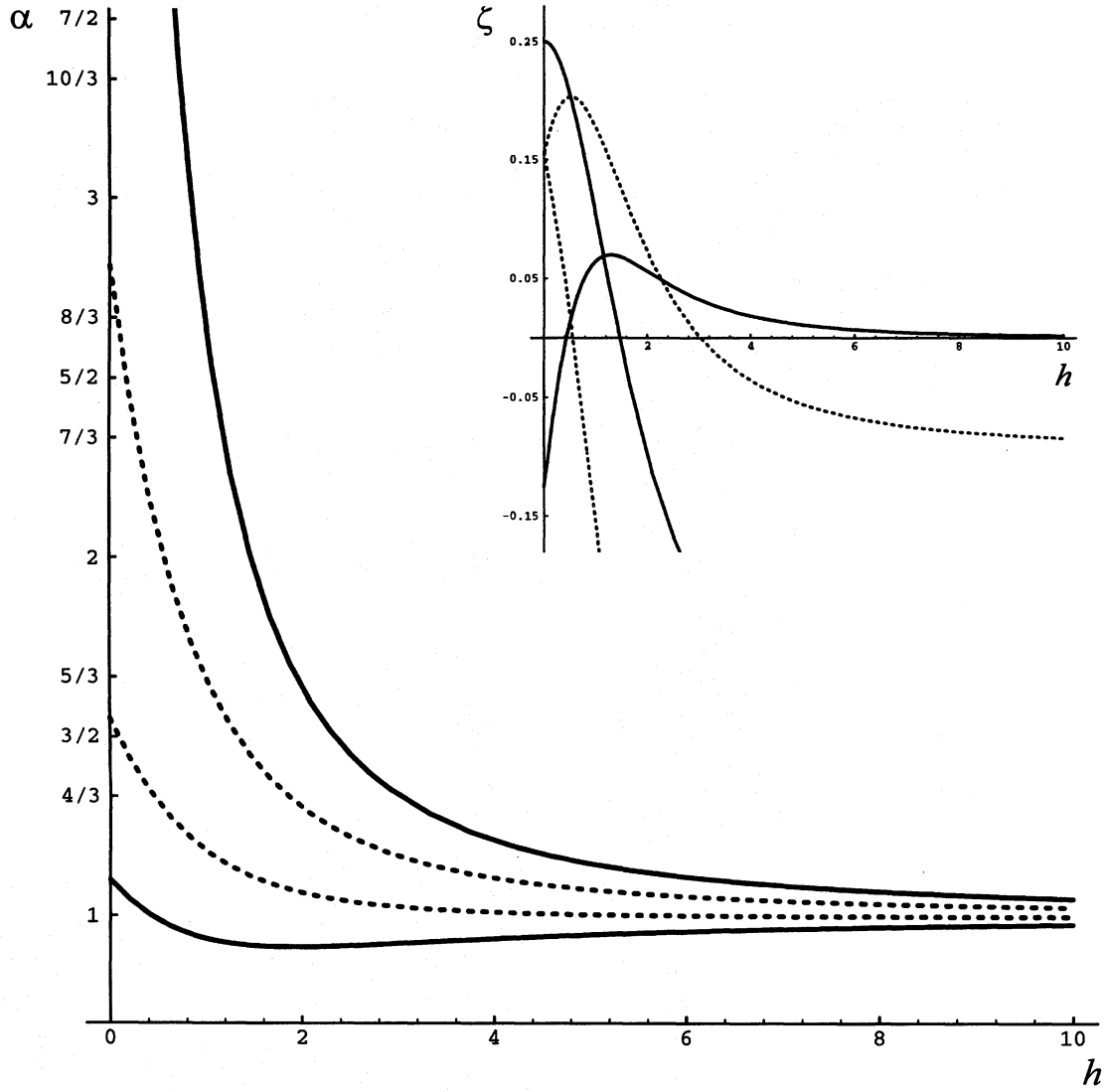

Figure 2. Cooperative resonances in the isochrone. The vertical axis is $\alpha=m/\ell$, while the abscissa is the angular momentum $h/\sqrt{GMb}$. The cooperation limit curves M_+ and M_- are plotted for two different values of the energy, $E=-8GM/b$ (dotted curves) and $E=-GM/8b$ (solid curves). See equations (3.7) and (3.11). At higher energies more resonances are cooperative. The plot inlayed in the upper right shows ζ as a function of h for fixed $E=-GM/8b$ and various α: $\alpha=2$ (upper solid curve), $\alpha=1$ (lower solid curve), $\alpha=4/3$ (upper dotted curve), and $\alpha=4$ lower dotted curve). At any fixed E, the global maxima of ζ is $1/4b^2$, which occurs for $\alpha=2$ and $h=0$ (bisymmetric radial orbits). For most resonances, the most cooperative orbits have low angular momentum.

3.2 Cooperation of nearly circular orbits

With equations (2.3) and (2.5) in hand, we see that the computation of the cooperation parameter ζ in particular models requires expressions for the fundamental frequencies $\Omega=(\partial H/\partial h)_{J_R}$ and $\kappa=(\partial H/\partial J_R)_h$ as functions of the actions h and J_R. Although expressions for Ω and κ cannot be found for a general axisymmetric potential, these frequencies can always be approximated to any given order in the amplitude a of the radial oscillation of the orbit. This is achieved using standard Hamiltonian perturbation theory (e.g., Born 1927, section 41), which has been widely used in diverse fields (see Donner 1979, chapter VI, for an application related to the present work). The results we need from this standard theory are simply quoted below; complete derivations are given by Earn (1993, section 4.3). The calculation described in this subsection gives ζ to lowest order, and hence determines the cooperative resonances for *nearly circular orbits* in an arbitrary axisymmetric potential.

It is useful to define an effective potential

$$U_{\rm eff}(R,h)=U(R)+\frac{h^2}{2R^2}, \tag{3.12}$$

and write the Hamiltonian

$$H=\frac{1}{2}v_R^2+U_{\rm eff}(R,h). \tag{3.13}$$

The guiding centre radius, $R_{\rm g}$, is defined implicitly as a function of angular momentum h, by centrifugal force gravity balance,

$$U_{\rm eff}^{(1)}(R_{\rm g})\equiv\left(\frac{\partial U_{\rm eff}}{\partial R}\right)_h(R_{\rm g})=\frac{{\rm d}U}{{\rm d}R}(R_{\rm g})-\frac{h^2}{R_{\rm g}^3}=0, \tag{3.14}$$

where in general we let $U_{\rm eff}^{(k)}(R_{\rm g})$ refer to the kth partial derivative of $U_{\rm eff}$ with respect to R at constant h, evaluated at $R=R_{\rm g}(h)$.

The perturbation calculation yields an azimuthal frequency,

$$\Omega_2=J_R\frac{{\rm d}\kappa_0}{{\rm d}h}+\frac{\rm d}{{\rm d}h}U_{\rm eff}(R_{\rm g}) \tag{3.15a}$$

$$=\Omega_0\left\{1+\frac{a^2}{R_{\rm g}^2}\left[\frac{3}{2}-6\frac{\Omega_0^2}{\kappa_0^2}+\frac{R_{\rm g}U^{(3)}(R_{\rm g})}{2\kappa_0^2}\right]\right\}, \tag{3.15b}$$

and a radial frequency,

$$\kappa_2=\kappa_0\left[1+\frac{a^2}{R_{\rm g}^2}\left\{\frac{15}{4}\frac{\Omega_0^2}{\kappa_0^2}-\frac{5}{48\kappa_0^4}\times[12\Omega_0^2-R_{\rm g}U^{(3)}(R_{\rm g})]^2+\frac{R_{\rm g}^2U^{(4)}(R_{\rm g})}{16\kappa_0^2}\right\}\right]. \tag{3.16}$$

To this order,

$$J_R=\frac{1}{2}\kappa_0a^2, \tag{3.17}$$

so equations (3.15) and (3.16) give the frequencies to first order in J_R. In these expressions,

$$\Omega_0=\frac{h}{R_{\rm g}^2}, \tag{3.18}$$

and

$$\kappa_0=[U_{\rm eff}^{(2)}(R_{\rm g})]^{1/2}. \tag{3.19}$$

Integer subscripts on Ω and κ refer here to the order of the frequency with respect to the amplitude a; these subscripts should not be confused with the subscript α on $\Omega_\alpha=\Omega-(1/\alpha)\kappa$.

We can now find an approximation for ζ by differentiation:

$$\zeta=\left(\frac{\partial\Omega_\alpha}{\partial h}\right)_{J_t}=\left(\frac{\partial}{\partial h}-\frac{1}{\alpha}\frac{\partial}{\partial J_R}\right)^2H=\frac{\partial\Omega}{\partial h}-\frac{2}{\alpha}\frac{\partial\Omega}{\partial J_R}+\frac{1}{\alpha^2}\frac{\partial\kappa}{\partial J_R}. \tag{3.20}$$

From equation (3.17) we have $a^2=2J_R/\kappa_0$. This allows us to write expressions (3.15b) and (3.16) directly in terms of J_R and h. We can then insert Ω_2 and κ_2 for Ω and κ in equation (3.20), perform the differentiations, and then finally discard the term containing J_R to obtain the leading-order behaviour of ζ. From equation (3.15a), we find

$$\left(\frac{\partial\Omega_2}{\partial h}\right)_{J_R=0}=\frac{{\rm d}^2}{{\rm d}h^2}U_{\rm eff}(R_{\rm g})=\frac{1}{({\rm d}h/{\rm d}R_{\rm g})^2}\left[U_{\rm eff}^{(2)}(R_{\rm g})-\frac{1}{{\rm d}h/{\rm d}R_{\rm g}}\frac{{\rm d}^2h}{{\rm d}R_{\rm g}^2}U_{\rm eff}^{(1)}(R_{\rm g})\right], \tag{3.21}$$

and

$$\frac{\partial\Omega_2}{\partial J_R}=\frac{{\rm d}\kappa_0}{{\rm d}h}=\frac{1}{2\kappa_0}\frac{{\rm d}\kappa_0^2}{{\rm d}R_{\rm g}}\frac{1}{{\rm d}h/{\rm d}R_{\rm g}}. \tag{3.22}$$

Equations (3.16) and (3.17) give

$$\frac{\partial\kappa_2}{\partial J_R}=\frac{15}{2}\frac{\Omega_0^2}{\kappa_0^2}-\frac{5}{24\kappa_0^4}[12\Omega_0^2-R_{\rm g}U^{(3)}(R_{\rm g})]^2+\frac{R_{\rm g}^2U^{(4)}(R_{\rm g})}{8\kappa_0^2}. \tag{3.23}$$

We can now use equations (3.21), (3.22) and (3.23) in equation (3.20) to write the leading-order behaviour of ζ as a function of $R_{\rm g}$ and derivatives with respect to $R_{\rm g}$. Since we are no longer interested in the fact that $R_{\rm g}$ can be written as a function of h, we now write R rather than $R_{\rm g}$.

A convenient expression for ζ can be found by introducing the dimensionless functions

$$\xi\equiv\frac{\kappa_0^2}{\Omega_0^2}=\frac{\partial\ln h^2}{\partial\ln R},\qquad \xi'\equiv\frac{\partial\xi}{\partial\ln R},\qquad \xi''\equiv\frac{\partial\xi'}{\partial\ln R}. \tag{3.24}$$

The cooperation parameter may then be written

$$\zeta = \frac{1}{\alpha^2 R^2}\left(\frac{\xi-4}{\xi}\right)(\alpha - M_-)(\alpha - M_+) + \mathscr{O}\left(\frac{a}{R}\right)^2. \tag{3.25a}$$

Here

$$M_\pm = \sqrt{\xi}\left[1 + \eta(\xi) \pm \sqrt{\frac{1}{12}[(\xi-1)+\eta(\xi)\mu(\xi)]}\right], \tag{3.25b}$$

where

$$\eta(\xi) = \frac{\xi'}{\xi(\xi-4)}, \tag{3.25c}$$

$$\mu(\xi) = \frac{1}{2}\left[14 + \xi + \eta(\xi)(5\xi+4) - 3\frac{\xi''}{\xi'}\right]. \tag{3.25d}$$

For $1 < \xi < 4$, the expression (3.25a) is positive only if α lies between M_- and M_+. Thus when a^2/R^2 is neglected the condition for cooperation of orbital streams is

$$\zeta > 0 \Leftrightarrow \begin{cases} M_- < \alpha < M_+, & \text{for } \xi < 4, \\ \alpha < M_- \text{ or } \alpha > M_+, & \text{for } \xi > 4. \end{cases} \tag{3.26}$$

We have carried the perturbation expansion through to fourth order in order to obtain the cooperation parameter to $\mathscr{O}(a^2/R^2)$, but the expression for ζ to this order is far too complicated to be useful, so we do not give it here.

3.3 Cooperation in power-law potentials

Condition (3.26) becomes simple when ξ is a constant, i.e., for power laws. If $v_c \propto R^\beta$, then

$$M_\pm = \sqrt{\xi}\left[1 \pm \sqrt{\frac{1}{12}(\xi-1)}\right], \tag{3.27a}$$

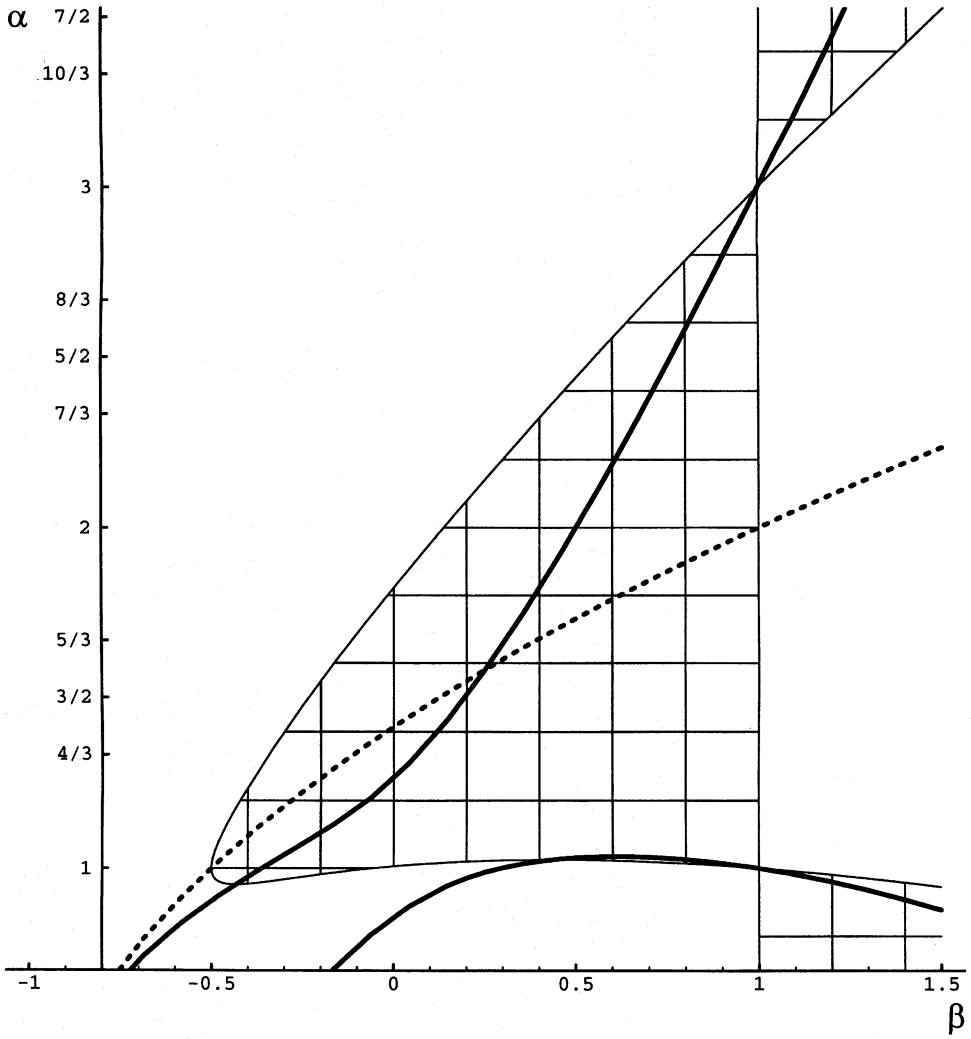

Figure 3. Cooperative resonances ($\alpha = m/\ell$) in power-law potentials. α is plotted vertically, and the horizontal axis is β, the power of the circular velocity law. The cooperative resonances ($\zeta > 0$) for nearly circular orbits lie in the hashed region of this figure ($\zeta = 0$ on the boundary of the hashed region). The dotted curve relates to the special power laws discussed in Section 3.4; it is defined by $\beta = (\alpha^2/2) - 1$, and shows that the resonance that determines the special power is cooperative provided $1 < \alpha < 2$. The heavy solid curves give the loci of extrema of $R^2\zeta$ at fixed α. The part of the figure near $\alpha = 1$ is shown on an expanded scale in Fig. 4.

$$\xi \equiv 2(\beta+1). \tag{3.27b}$$

The cooperative region (3.26) is hashed in Fig. 3. The dimensionless cooperation parameter $R^2\zeta$ is never very large for power laws. Its maximum is 0.091 3064, for $\alpha = 1.315\,93$ (near 4/3) and $\beta = 0.049\,0381$. For the $\alpha = 2$ resonance the maximum of $R^2\zeta$ is 0.035 6836 at $\beta = 0.500\,184$, while for the $\alpha = 1$ resonance its maximum is 0.026 7948 at $\beta = -0.361\,589$. For any chosen resonance α, the extreme values of $R^2\zeta$ occur when ξ satisfies

$$\alpha = \frac{1}{8}\sqrt{\xi}\left\{4+\xi \pm \sqrt{\frac{1}{3}[11(\xi-2)^2+4)]}\right\}. \tag{3.28}$$

The locus of such points defines the two heavy solid curves in Fig. 3. The higher of the two corresponds to maximum ζ at fixed α and the lower to minimum. The lower heavy solid curve intersects the lower boundary (M_-) of the cooperative region when $\beta = \sqrt{3}/4$ and $\beta = 1$. Thus if the minimum ζ at fixed α is positive then it occurs for $\beta \geq \sqrt{3}/4 \simeq 0.433\,013$ (and very near to $\alpha = 1$ when $\beta \leq 1$, which is always true in galaxies). The behaviour of the curves is difficult to see near $\alpha = 1$, so this region is expanded in Fig. 4.

3.4 Kinematically cooperative models

Since the cooperation mechanism operates on resonant and near-resonant orbits, we would expect it to be most effective if all orbits happened to be resonant. We therefore consider special potentials in which all nearly circular orbits are α-symmetric in the same frame. We say that such models are *kinematically cooperative*, because in the absence of self-gravity an α-symmetric pattern can be sustained indefinitely; the usual winding of kinematic density waves (Kalnajs 1973; Binney & Tremaine 1987, section 6.2.1) does not occur in these models.

As seen from fixed axes, a closed orbital stream will typically tumble over and over. To make a permanent configuration from many such streams they must all tumble at the same rate. So to build up an α-symmetric pattern that rotates rigidly with angular velocity Ω_p, we must have $\Omega_\alpha = \Omega_p$ for orbits with a whole range of guiding centre radii. We consider here the most extreme case, in which $\Omega_\alpha = \Omega_p$ for *all* nearly circular orbits; from the solutions we derive, models that are kinematically cooperative only in restricted regions can also be constructed.

Writing κ_0 as a function of Ω_0 (e.g., Binney & Tremaine 1987, equation 3.59) we may express the condition $\Omega_\alpha = \Omega_p$ (for nearly circular orbits) as a differential equation:

$$4\Omega_0^2 + R\frac{\mathrm{d}\Omega_0^2}{\mathrm{d}R} = \alpha^2(\Omega_0 - \Omega_p)^2. \tag{3.29}$$

This equation and its general solutions were first derived by Berry (1973). A systematic analysis of these solutions is given by Earn (1993).

3.4.1 *Non-rotating patterns*

In the simplest case $\Omega_p = 0$, so the α-symmetric patterns do not rotate. Equation (3.29) is then trivial and yields a power law

$$\Omega_0 \propto R^{(\alpha^2/2)-2},$$

or

$$v_c \propto R^{(\alpha^2/2)-1}.$$

In the special case $\alpha = 3/2$ (so $v_c \propto R^{1/8}$), all nearly circular orbits will have trefoil symmetry and will close after two

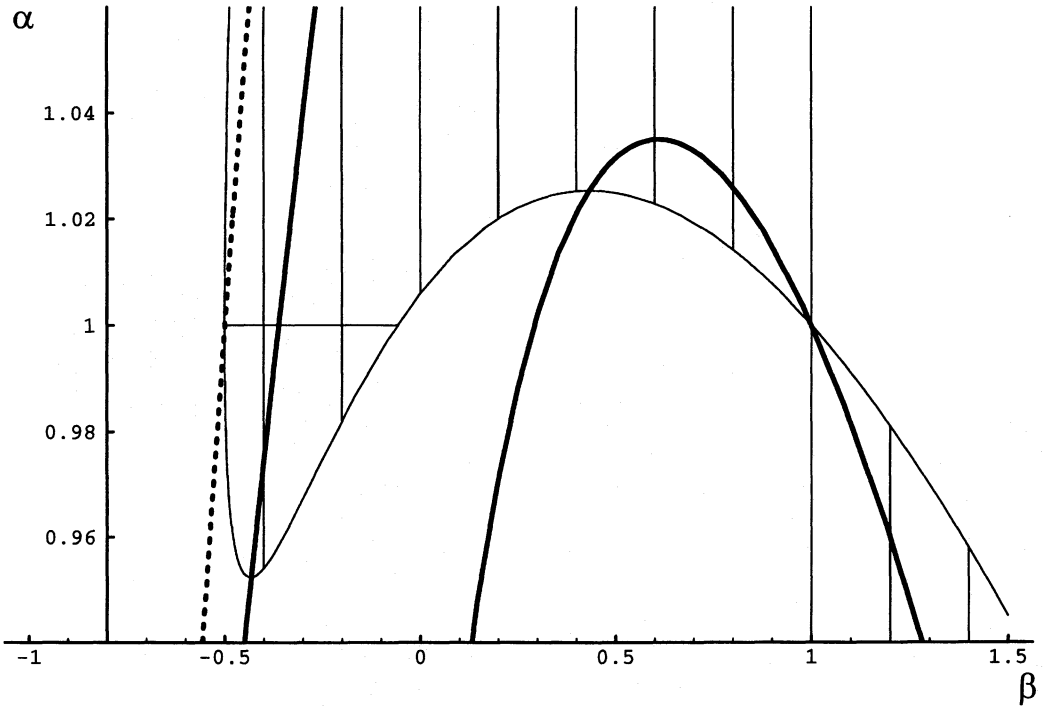

Figure 4. A vertically expanded view of the region near the $\alpha = 1$ resonance in Fig. 3.

turns around the origin. This, and the case $\alpha = 4/3$ ($v_c \propto R^{-1/9}$), are especially interesting, because they give rise to rotation curves that are nearly flat, similar to observed rotation curves. Thus in galaxies with flat rotation curves, three- and four-fold symmetric patterns can be sustained even without help from self-gravity.

Fig. 3 shows that when self-gravity is taken into account, these velocity laws are always cooperative for the resonance of interest, provided that $-1/2 < \beta < 1$, i.e., $1 < \alpha < 2$. In Fig. 3 the relation $\beta = \alpha^2/2 - 1$ is shown by the dotted curve, which goes exactly through the middle of the cooperative region since $\beta = \alpha^2/2 - 1$ is equivalent to

$$\alpha = \sqrt{2(\beta+1)} = \sqrt{\xi} = (M_+ + M_-)/2.$$

Cooperation ends at the $\beta = -1/2$ (Kepler) and $\beta = 1$ (simple harmonic) cases. For all the special cases in which $\beta = \alpha^2/2 - 1$, the dimensionless cooperation parameter has a very simple form:

$$R^2\zeta = \frac{(\alpha^2-1)(4-\alpha^2)}{12\alpha^2}. \tag{3.30}$$

In summary, for non-rotating patterns, kinematic cooperation leads to dynamic cooperation.

3.4.2 *Rotating patterns*

With $\Omega_p \neq 0$, equation (3.29) is more complicated, but it can be separated and written as

$$\int \frac{dR}{R} = \int \frac{2\Omega_0/\Omega_p^2}{[(|\alpha|+2)\Omega_0/\Omega_p - |\alpha|]\,[(|\alpha|-2)\Omega_0/\Omega_p - |\alpha|]}\, d\Omega_0. \tag{3.31}$$

This integral is elementary, but $|\alpha| = 2$ is a special case. Writing R_p for the radius at which $\Omega_0 = \Omega_p$, we obtain

$$\frac{R}{R_p} = \begin{cases} \dfrac{\left|\left(\dfrac{|\alpha|}{2}-1\right)\dfrac{\Omega_0}{\Omega_p} - \dfrac{|\alpha|}{2}\right|^{\frac{1}{2(|\alpha|-2)}}}{\left|\left(\dfrac{|\alpha|}{2}+1\right)\dfrac{\Omega_0}{\Omega_p} - \dfrac{|\alpha|}{2}\right|^{\frac{1}{2(|\alpha|+2)}}}, & \text{if } |\alpha| \neq 2, \\ \dfrac{1}{e^{\frac{1}{4}\left(\frac{\Omega_0}{\Omega_p}-1\right)}\left|2\dfrac{\Omega_0}{\Omega_p}-1\right|^{1/8}}, & \text{if } |\alpha| = 2. \end{cases} \tag{3.32}$$

This implicit relation gives 11 distinct behaviours for $\Omega_0(R)$, seven of which can be rejected because $|\Omega_0|$ increases as a function of R (Earn 1993). This leaves us with four qualitatively different physical cases. In Fig. 5 we show $v_c = R\Omega_0$ (solid curve), Ω_0 (dashed curve) and $\kappa_0 = \alpha(\Omega_0 - \Omega_p)$ (dotted curve) for each of these cases. An example of a long-lived kinematic density wave in the model of Fig. 5(c) ($|\alpha| = 2$) is shown in Fig. 6.

Fig. 5 reveals a peculiarity of these models that deserves comment. In a spherically symmetric model, $\nabla^2[U(r)] = \kappa_0^2 - \Omega_0^2$, so the mass density $\rho(r) > 0$ if and only if $\kappa_0 > \Omega_0$. This condition does not hold in non-spherical systems such as the flat disc of interest here, but the fact that $\kappa_0 < \Omega_0$ in some regions of the rotating kinematically cooperative models is unusual, and raises the concern that they may involve negative surface densities. The important point, which we wish to stress, is that it is easy to construct rotating discs that are kinematically cooperative over large radial ranges and have non-negative surface density everywhere. To see this, consider a finite disc obtained by squashing the finite sphere of radius r_0 with density $\rho(r)$. For $R \leq r_0$, the surface density of the disc is

$$\Sigma(R) = 2\int_0^{\sqrt{r_0^2-R^2}} \rho(r)\, dz, \tag{3.33}$$

where $r = \sqrt{R^2+z^2}$ is the spherical radius. We may rewrite this as

$$\Sigma(R) = \frac{1}{2\pi G}\int_R^{r_0} \frac{\kappa_0^2(r) - \Omega_0^2(r)}{\sqrt{r^2-R^2}}\, r\, dr \tag{3.34a}$$

$$= \frac{1}{2\pi G}\int_{\Omega_0(R)}^{\Omega_0(r_0)} \frac{\kappa_0^2(\Omega_0) - \Omega_0^2}{\sqrt{r^2(\Omega_0)-R^2}}\, r(\Omega_0)\, \frac{dr}{d\Omega_0}\, d\Omega_0, \tag{3.34b}$$

and the integration interval $[R, r_0]$ can be divided into regions where we know $\Omega_0(r)$ or $r(\Omega_0)$. In kinematically cooperative regions, $\kappa_0^2(\Omega_0) = [\alpha(\Omega_0 - \Omega_p)]^2$, and equation (3.32) gives $r(\Omega_0)$. In all the models presented in Fig. 5, $\kappa_0^2 - \Omega_0^2$ approaches a positive constant as $R \to \infty$ (cf. Earn 1993, table 2.1); hence if a sufficiently large r_0 is taken, equation (3.34) will yield $\Sigma(R) > 0$ everywhere even for strictly kinematically cooperative models. More realistic models can be constructed that are kinematically cooperative in extensive regions.

Our general formula (3.25) for ζ for nearly circular orbits is local in R, but it turns out that for the kinematically cooperative models, the sign of ζ is the same everywhere. We can therefore make a general statement about (dynamic) cooperation in kinematically cooperative regions without worrying about exactly what radial intervals of equation (3.32) have been included in a particular disc model.

Computing ζ from equation (3.32) is a messy affair. To evaluate the expression in (3.25) directly, we need Ω_0 as a function of R (since ξ is a function of Ω_0 and the derivatives in equation 3.25 are with respect to R). Instead, we have only the expression (3.32) for R as a function of Ω_0. To find the leading-order behaviour of ζ for these models, equation (3.25) must be re-expressed in terms of derivatives with respect to Ω_0, via

$$\frac{d}{d\ln R} = \left(\frac{d\ln R}{d\Omega_0}\right)^{-1}\frac{d}{d\Omega_0}, \tag{3.35}$$

and so on. [This transformation is valid along each one-to-one branch of the solution function $R(\Omega_0)$.] We are left with an extremely tedious calculation. Note that since $\Omega_0 - (1/\alpha)\kappa_0 \equiv \Omega_p$ in these models, a number of the terms in the expression for ζ cancel out. Even so, the resulting formulae are so ugly that giving them here would be pointless. The lengthy but straightforward nature of this calculation makes it well-suited to the MATHEMATICA system (Wolfram 1991), which we have used to write a program that evaluates equations (3.25) for given functions $R(\Omega_0)$. The MATHEMATICA program was tested by expressing R as a function of Ω_0 for

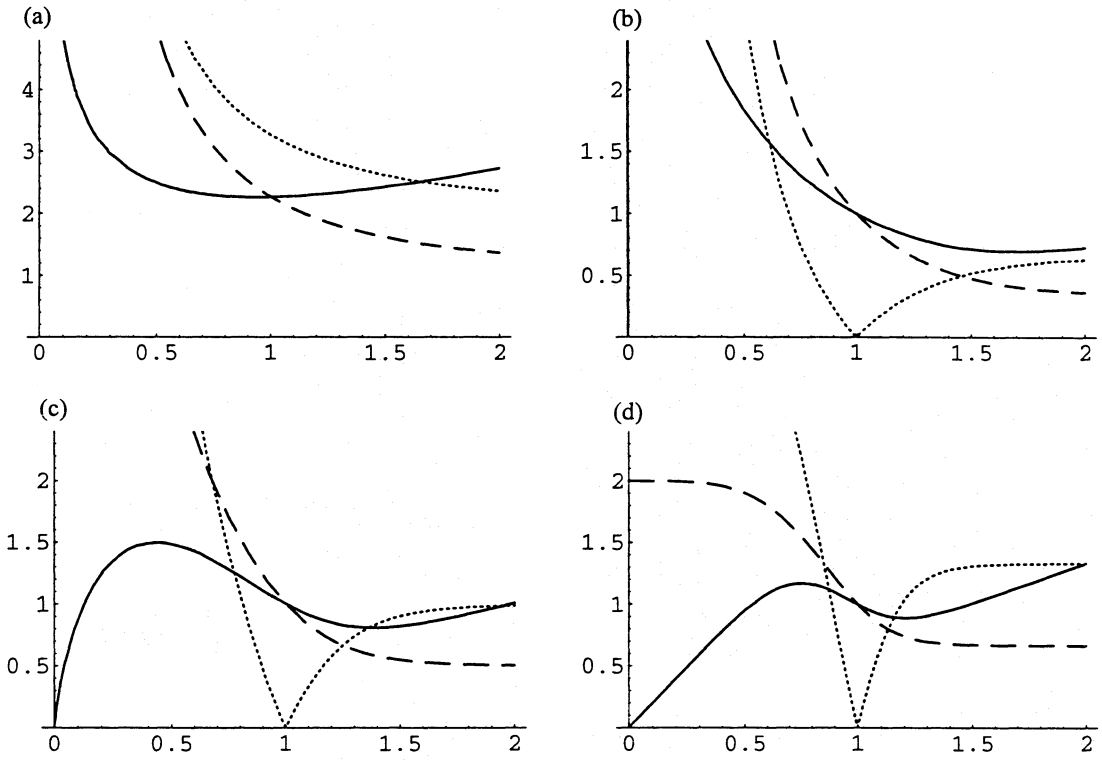

Figure 5. Physical solutions derived from equation (3.32). In each panel, the solid curve is the rotation curve $v_c(R)$ in units of $R_p\Omega_p$. The dashed curve is $\Omega(R)$. The dotted curve is $\kappa(R)$. Panel (a) gives the rotation curve for a backward-rotating ($\Omega_p < 0$) lopsided pattern; $\kappa - \Omega$ is constant at the value 1 in the units of the figure. Panel (b) is for a forward-rotating ($\Omega_p > 0$) lopsided pattern. $\Omega - \kappa$ is constant for $R < R_p$ and $\Omega + \kappa$ is constant for $R > R_p$. (c) $|\alpha| = 2$, relevant for bars or two-arm spirals; $\Omega - (1/2)\kappa$ is constant for $R < R_p$ and $\Omega + (1/2)\kappa$ is constant for $R > R_p$. (d) $|\alpha| = 4$, constant 4:1 resonance.

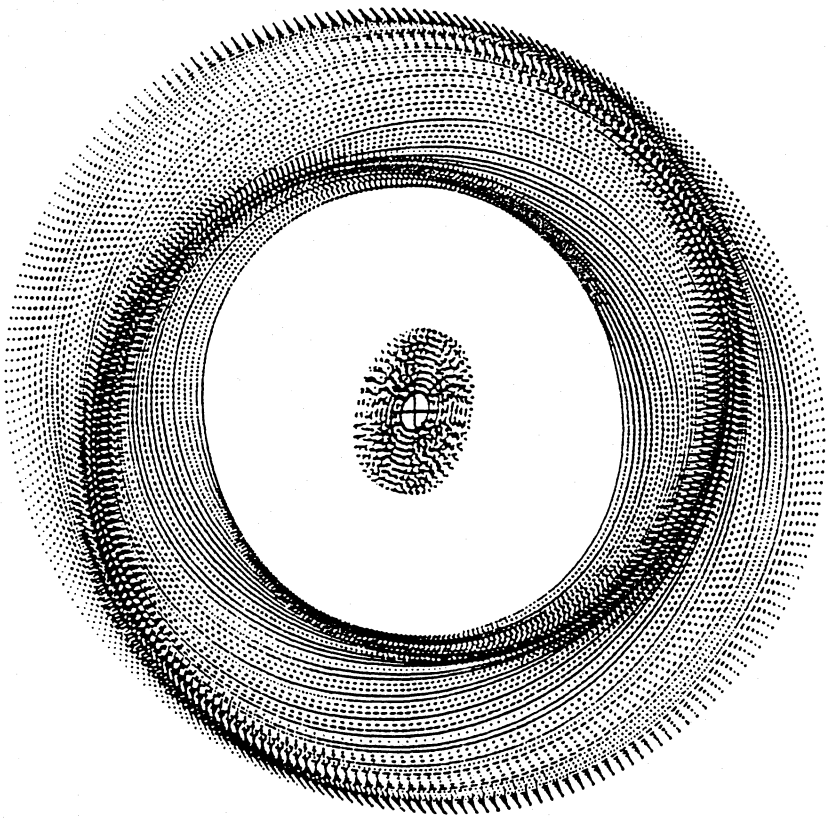

Figure 6. A rotating bisymmetric pattern of orbits in the model of Fig. 5(c). In the 'bar' $\alpha = 2$, whereas in the spiral $\alpha = -2$.

the isochrone and reproducing the results available from equation (3.6).

In these kinematically cooperative models that support rotating α-symmetric patterns self-gravity brings one surprise: the $\alpha = 1$ resonance is *not* cooperative *anywhere* for the model in Fig. 5(a) (backward-rotating pattern). However, $\alpha = 1$ *is* cooperative *everywhere* in Fig. 5(b) (forward-rotating pattern). In Fig. 5(c), $\alpha = 2$ *is* cooperative everywhere and the same is true of the $\alpha = 4$ resonance in Fig. 5(d).

4 DISCUSSION

We have derived several results that can be used to quantify the level of cooperation (for any resonance α) implied by observed rotation curves. Fig. 3 makes it possible to estimate the cooperation parameter ζ for nearly circular orbits in a region of a galaxy by fitting a local power law to the rotation curve. In general, equation (3.25) gives ζ for nearly circular orbits in any axisymmetric disc. Alternatively, if orbits of a galactic potential can be well-fitted with a generalized isochrone (cf. Evans et al. 1990, appendix A) then equation (3.6) permits a general discussion of cooperation in the galaxy. A full cooperation analysis for an arbitrary model would need to be done numerically.

In his study of the dynamics of barred galaxies, Lynden-Bell (1979) had already found that the isochrone potential is cooperative for $\alpha = 2$, from the centre to well beyond the maximum in the rotation curve, which occurs at $R = 2.20b$ (the exact guiding-centre radius at which ζ changes sign depends on the orbital eccentricity, but is $R_g = 3.73b$ for nearly circular orbits). The inner region of the isochrone approximates the simple harmonic oscillator potential, which supports *non-rotating* $\alpha = 2$-symmetric patterns. Since the $\alpha = 2$ resonance is neither cooperative nor uncooperative in the harmonic potential, it is not surprising that a small change in the potential can make $\alpha = 2$ cooperative; but since $\Omega - (1/2)\kappa$ remains *small* when changing from the harmonic oscillator to the isochrone, the expected pattern speed of *zero* is not increased by much. However, as first shown by Lindblad (1956) the relation $\Omega - (1/2)\kappa = \Omega_p$, with non-negligible Ω_p, holds approximately in the inner parts of typical galactic discs. This is the condition that defines the kinematically cooperative model shown in Fig. 5(c) (for $R \leq R_p$); since we have found that this model is (dynamically) cooperative for $\alpha = 2$ nearly circular orbits everywhere, it follows that in principle, galaxies can sustain fast rotating bars by the cooperation mechanism. Judging from the isochrone (Fig. 2) we expect $\alpha = 2$ cooperation to be more effective for more eccentric orbits and hence to have a greater influence after a weak bar has already formed.

In the case of lopsidedness self-gravity may be a small effect. In the outer region of disc galaxies, where lopsidedness is most pronounced, the mass attributable to the observed matter (mostly neutral hydrogen gas) typically accounts for only a fraction of the mass inferred from the rotation curve, usually no more than 25 per cent (e.g., Casertano & van Albada 1990). If the gravitational potential of the galaxy is dominated by a dark halo in these parts then observed lopsided density waves could be approximately kinematic. [We remark that the observational signature of lopsided kinematic density waves is a rotation curve that is systematically higher on the shorter side (Earn 1993, section 2.6).] If $\alpha = 1$ is cooperative in the relevant region of the given galaxy then self-gravity will tend to help lopsided ($\alpha = 1$-symmetric) density waves to live for a long time. As mentioned above, this is not the case for the peculiar potential that sustains backward-rotating, kinematic, $\alpha = 1$-symmetric patterns forever (Fig. 5a). However, $\alpha = 1$ is cooperative in the outer parts of the isochrone (beyond the rotation curve maximum) and everywhere in power laws with $v_c \propto R^\beta$, $-0.5 < \beta \lesssim -0.0584$; so in some similar models self-gravity tends to compensate for the fact that $\Omega - \kappa$ is not exactly constant (but is negative and small).

Lynden-Bell (1979) envisaged that the cooperation mechanism could be responsible for the formation of bars through (linear) gravitational instabilities. Palmer & Papaloizou (1987) have shown that this does seem to be the physical origin of the radial orbit instability in spherical systems. In flat discs, however, where most orbits are nearly circular, cooperation of orbital streams does not seem to be the trigger of (linear) bar formation, as we discuss below. This conclusion might be guessed from the example of the isochrone (Fig. 2) in which ζ has significant magnitude only for nearly radial orbits.

We can identify three distinct mechanisms that are associated with the cooperation parameter and could trigger the growth of unstable bar modes in discs: (i) cooperative orbit alignment ($\alpha = 2$, $\zeta > 0$) similar to the Jeans instability for individual stars (Lynden-Bell 1979) – in this case we would expect a strong correlation between the sign of the $\alpha = 2$ cooperation parameter and the formation of a bar in a disc model; (ii) uncooperative anti-alignment of orbits ($\alpha = 2$, $\zeta < 0$) similar to the two-stream instability of plasma physics (Collett 1988) – here an anticorrelation would be expected between bar formation and the sign of ζ for $\alpha = 2$; (iii) non-cooperation at corotation ($m = 2$ but $\alpha \to \infty$, $\zeta < 0$) (Collett 1994). Two-stream instability probably works most powerfully on the $m = 2$ disturbances of material near corotation where all the little Lindblad epicycles are uncooperative.

A decisive test for mechanisms (i) and (ii) is the stability analyses of scale-free (power-law) discs in which the sign of the cooperation parameter is the same everywhere. Earn (1993) has studied the linear stability of a class of power-law discs (Evans 1994) and found no correlation (or anticorrelation) between instability of bar modes and the sign of the $\alpha = 2$ cooperation parameter (Fig. 3 of this paper): nor did he find a relation between lopsided instabilities and the sign of the $\alpha = 1$ cooperation parameter. This appears to eliminate mechanisms (i) and (ii) in the linear regime, although it says nothing about mechanism (iii) because corotation is *always* uncooperative, so two-stream instability could work whenever there was a deep enough minimum in the effective distribution function.

This indicates that cooperative alignment of orbits does not drive typical linear bar instabilities in stellar discs. Another mechanism must be responsible, perhaps mechanism (iii), but in any case presumably one that causes unstable modes to grow faster than bisymmetric orbits can be trapped. Orbital alignment instabilities with small growth rates may still exist, but if they are masked by more virulent instabilities then they are irrelevant.

Nevertheless, there are several ways in which cooperation of orbital streams may be important in the evolution of real disc galaxies. In particular, if galactic discs are typically more

stable than models that are easy to construct, then the unstable modes may grow slowly enough that the fast action is adiabatically invariant and the cooperation mechanism governs the growth. Alternatively, encounters with other galaxies can excite linearly stable discs, perhaps to high enough amplitude for non-linear effects to take over; the cooperation analysis is still valid in this circumstance, as we now explain.

The cooperation analysis is valid provided that the perturbation V to the *potential* is small. In contrast, the linearized collisionless Boltzmann equation is valid only while the perturbation f to the *phase-space density* is small. Since V is obtained from f by four or six integrations, it is greatly smoothed compared with f and the cooperation analysis will be valid well into the non-linear regime (in the sense of the Boltzmann equation).

One way we plan to explore the significance of cooperation for the non-linear evolution of discs is to compare the non-linear behaviour of two bar-forming models with cooperation parameters of opposite sign. Models with very massive haloes should also be explored carefully, since the growth rates of unstable modes will tend to be lower.

The true origin of bars, lopsidedness and other non-axisymmetric features in disc galaxies is not clear. However, some bars may be formed by interaction of galaxies that were not formerly barred. We therefore note finally that angular momentum loss to a passing perturber, from particles of a ring near inner Lindblad resonance with it, inevitably leads to an increase of $J_f/h = 1/2 + J_R/h$. This increase in J_R/h entails an increase in the rings' ellipticity (Lynden-Bell 1963) so forming a bar shape, and moreover, typically making cooperation more effective. Whatever the process of pattern formation, we emphasize again that cooperation may be important for *sustaining* non-axisymmetric features for a long time.

ACKNOWLEDGMENTS

We thank the anonymous referee for helpful comments. DE is grateful for support from a United Kingdom Commonwealth Scholarship and a Lady Davis Postdoctoral Fellowship.

REFERENCES

Arnold V. I., Kozlov V. V., Neishtadt A. I., 1988, in Arnold V. I., ed., Dynamical Systems III, Encyclopedia of Mathematical Sciences 3. Springer-Verlag, Berlin
Arnold V. I., 1989, Mathematical Methods of Classical Mechanics, 2nd edn. Springer-Verlag, Berlin
Berry C. L., 1973, ApJ, 179, 395
Binney J. J., Tremaine S., 1987, Galactic Dynamics. Princeton Univ. Press, Princeton
Born M., 1927, The Mechanics of the Atom. Frederick Ungar, New York
Casertano S., van Albada T. S., 1990, in Lynden-Bell D., Gilmore G., eds, Baryonic Dark Matter. Kluwer, Dordrecht, p. 159
Collett J. L., 1988, unpublished
Collett J. L., 1994, unpublished
Donner K. J., 1979, PhD thesis, Cambridge Univ.
Earn D. J. D., 1993, PhD thesis, Cambridge Univ.
Evans N. W., 1994, MNRAS, 267, 333
Evans N. W., de Zeeuw P. T., Lynden-Bell D., 1990, MNRAS, 244, 111
Goldstein H., 1980, Classical Mechanics, 2nd edn. Addison-Wesley, New York
Hénon M., 1959, Ann d'Astrophys., 33, 126
Kalnajs A. J., 1973, Proc. Astron. Soc. Aust., 2, 174
Lichtenberg A. J., Lieberman M. A., 1992, Regular and Chaotic Dynamics, 2nd edn. Springer-Verlag, Berlin
Lindblad B., 1956, Stockholm Obs. Ann., 19, 7
Lynden-Bell D., 1963, The Observatory, 83, 23
Lynden-Bell D., 1979, MNRAS, 187, 101
Lynden-Bell D., Kalnajs A. J., 1972, MNRAS, 157, 1
Palmer P. L., Papaloizou J., 1987, MNRAS, 224, 1043
Wolfram S., 1991, Mathematica: A System for Doing Mathematics by Computer, 2nd edn. Addison-Wesley, New York